Metabolism 145 (2023) 155630

Contents lists available at ScienceDirect

Metabolism

journal homepage: www.journals.elsevier.com/metabolism

Protective effects of the succinate/SUCNR1 axis on damaged hepatocytes in NAFLD

Anna Marsal-Beltran [a,b,c], Adrià Rodríguez-Castellano [a,c], Brenno Astiarraga [a,b], Enrique Calvo [a,b,1], Patricia Rada [b,d], Ana Madeira [a,b], M-Mar Rodríguez-Peña [a,b], Gemma Llauradó [b,e], Catalina Núñez-Roa [a,b], Beatriz Gómez-Santos [f], Elsa Maymó-Masip [a,b], Ramon Bosch [g], María Dolores Frutos [h], José María Moreno-Navarrete [i,j], Bruno Ramos-Molina [k], Patricia Aspichueta [f,l,m], Jorge Joven [c,n], José-Manuel Fernández-Real [i,j], Juan Carlos Quer [a,c], Ángela M. Valverde [b,d], Albert Pardo [a,c], Joan Vendrell [a,b,c], Victòria Ceperuelo-Mallafré [a,b,c,*], Sonia Fernández-Veledo [a,b,c,*]

[a] *Hospital Universitari Joan XXIII de Tarragona, Institut d'Investigació Sanitària Pere Virgili (IISPV), 43005 Tarragona, Spain*
[b] *CIBER de Diabetes y Enfermedades Metabólicas Asociadas (CIBERDEM)-Instituto de Salud Carlos III (ISCIII), 28029, Madrid, Spain*
[c] *Universitat Rovira i Virgili (URV), 43201 Reus, Spain*
[d] *Instituto de Investigaciones Biomédicas Alberto Sols (CSIC-UAM), 28029 Madrid, Spain*
[e] *Department of Endocrinology and Nutrition, Hospital del Mar, Institut Hospital del Mar d'Investigacions Mèdiques (IMIM), 08003 Barcelona, Spain*
[f] *Department of Physiology, Faculty of Medicine and Nursing, University of the Basque Country UPV/EHU, 48940 Leioa, Spain*
[g] *Department of Pathology, Oncological Pathology and Bioinformatics Research Group, Hospital de Tortosa Verge de la Cinta – IISPV, 43500 Tortosa, Spain*
[h] *Department of General and Digestive System Surgery, Virgen de la Arrixaca University Hospital, 30120 Murcia, Spain*
[i] *Department of Diabetes, Endocrinology and Nutrition and Institut d'Investigació Biomèdica de Girona (IDIBGI), Dr. Josep Trueta University Hospital, Department of Medicine, University of Girona, 17007 Girona, Spain*
[j] *CIBER de Fisiopatología de la Obesidad y Nutrición (CIBEROBN) - Instituto de Salud Carlos III, 28029 Madrid, Spain*
[k] *Obesity and Metabolism Laboratory, Biomedical Research Institute of Murcia (IMIB), 30120 Murcia, Spain*
[l] *Biocruces Bizkaia Health Research Institute, 48903 Barakaldo, Spain*
[m] *CIBER de Enfermedades Hepáticas y Digestivas (CIBEREHD)- Instituto de Salud Carlos III (ISCIII), 28029 Madrid, Spain*
[n] *Unitat de Recerca Biomèdica, Hospital Universitari de Sant Joan, Institut d'Investigació Sanitària Pere Virgili, 43204 Reus, Spain*

ARTICLE INFO

Keywords:
Succinate
SUCNR1
NASH
Steatosis
Hepatocyte
Glycogen

ABSTRACT

Objective: Succinate and succinate receptor 1 (SUCNR1) are linked to fibrotic remodeling in models of non-alcoholic fatty liver disease (NAFLD), but whether they have roles beyond the activation of hepatic stellate cells remains unexplored. We investigated the succinate/SUCNR1 axis in the context of NAFLD specifically in hepatocytes.

Methods: We studied the phenotype of wild-type and *Sucnr1*$^{-/-}$ mice fed a choline-deficient high-fat diet to induce non-alcoholic steatohepatitis (NASH), and explored the function of SUCNR1 in murine primary hepatocytes and human HepG2 cells treated with palmitic acid. Lastly, plasma succinate and hepatic *SUCNR1* expression were analyzed in four independent cohorts of patients in different NAFLD stages.

Results: Sucnr1 was upregulated in murine liver and primary hepatocytes in response to diet-induced NASH. *Sucnr1* deficiency provoked both beneficial (reduced fibrosis and endoplasmic reticulum stress) and detrimental (exacerbated steatosis and inflammation and reduced glycogen content) effects in the liver, and disrupted

Abbreviations: ACC, acetyl-CoA carboxylase; AMPKα, AMP-activated protein kinase subunit alpha; ASM, acid-soluble metabolites; ATF6, activating transcription factor 6; α-SMA, alpha-smooth actin; CD-HFD, choline-deficient high-fat diet; CHD, chow diet; CHOP, C/EBP-homologous protein; Col1a1, Collagen type I alpha 1; CREB, cAMP response element binding protein; EIF2α, alpha subunit of eukaryotic initiation factor 2; ER, endoplasmic reticulum; FAS, fatty acid synthase; GAPDH, glyceraldehyde-3phosphate dehydrogenase; GS, glycogen synthase; GSK3α/β, glycogen synthase kinase 3 alpha/beta; HFD, high-fat diet; HSCs, hepatic stellate cells; IRE-1, inositol-requiring enzyme 1; PA, palmitic acid; PKA-C, protein kinase A subunit C; PPARG, peroxisome proliferator-activated receptor gamma; SREBF1, sterol regulatory element binding transcription factor 1; SUCNR1, succinate receptor 1; Tnf, tumor necrosis factor alpha.

* Corresponding authors at: Research Unit, University Hospital of Tarragona Joan XXIII, C/ Dr. Mallafré Guasch, 4, 43005 Tarragona. Spain.
E-mail addresses: victoria.ceperuelo@urv.cat (V. Ceperuelo-Mallafré), sonia.fernandez@iispv.cat (S. Fernández-Veledo).
[1] Present address: Universitat Rovira i Virgili, Department of Biochemistry and Biotechnology, Nutrigenomics Research Group, 43007 Tarragona, Spain.

https://doi.org/10.1016/j.metabol.2023.155630
Received 24 February 2023; Accepted 9 June 2023
Available online 13 June 2023

glucose homeostasis. Studies *in vitro* revealed that hepatocyte injury increased *Sucnr1* expression, which when activated improved lipid and glycogen homeostasis in damaged hepatocytes. In humans, *SUCNR1* expression was a good determinant of NAFLD progression to advanced stages. In a population at risk of NAFLD, circulating succinate was elevated in patients with a fatty liver index (FLI) ≥60. Indeed, succinate had good predictive value for steatosis diagnosed by FLI, and improved the prediction of moderate/severe steatosis through biopsy when added to an FLI algorithm.

Conclusions: We identify hepatocytes as target cells of extracellular succinate during NAFLD progression and uncover a hitherto unknown function for SUCNR1 as a regulator of hepatocyte glucose and lipid metabolism. Our clinical data highlight the potential of succinate and hepatic SUCNR1 expression as markers to diagnose fatty liver and NASH, respectively.

1. Introduction

Non-alcoholic fatty liver disease (NAFLD) is the most common form of chronic liver disease in western countries and evolves in a scenario of metabolic dysfunction closely associated with obesity, type 2 diabetes mellitus (T2D) and cardiovascular disease [1]. Its progression from simple steatosis to more advanced phases such as non-alcoholic steatohepatitis (NASH), cirrhosis, and hepatocellular carcinoma involves multiple "hits", including lipotoxicity, oxidative stress, inflammation and gut microbiome dysfunction [2]. Although many agents can target these concurrent hits, no pharmacological therapies are currently approved for NAFLD [3]. Liver biopsy remains the gold standard in the evaluation of the course of NASH, despite limitations in its interpretation and inherent risks of the procedure, and diagnosis of its more severe forms is routinely performed by grading inflammation and staging fibrosis [4]. Accordingly, there is an urgent need for novel therapeutic strategies and noninvasive biomarkers for managing NAFLD.

We recently showed that succinate, a metabolite derived from both mitochondrial activity and bacterial metabolism, is a promising circulating biomarker for the early detection of metabolic dysfunction in obesity [5], T2D [6], and cardiovascular disease [7]. In the context of NAFLD, specific studies in patient cohorts are scarce and limited in size; however, elevated levels of circulating succinate have been reported in initial [8] and advanced [9] stages of the disease. Succinate belongs to a specific group of metabolites with signaling properties and functions as an extracellular ligand by binding its cognate receptor, succinate receptor 1 (SUCNR1), in a cell-specific manner [10]. Succinate thus acts akin to hormones and cytokines in regulating myriad biological processes.

Recent studies have shed light on the role of the succinate/SUCNR1 axis in both physiological and non-physiological processes, including its function in modulating the inflammatory response [11–13], the renin-angiotensin system in kidney [14], lipolysis in adipose tissue [15], and skeletal muscle remodeling [16]. Results from the few studies exploring the succinate/SUCNR1 axis in liver have described that *Sucnr1* is primarily expressed in hepatic stellate cells (HSCs) and activates fibrotic remodeling in cell culture and rodent models of NAFLD [17–22] in response to succinate secreted by hepatocytes. This suggests that blocking SUCNR1 could be an anti-fibrotic treatment for NAFLD [23]. However, the contribution of SUCNR1 signaling in other liver cell populations has not been explored, and it is unknown whether SUCNR1 might also modulate hepatic glucose homeostasis, steatosis, and inflammation.

We used mice with global *Sucnr1* deletion together with primary hepatocytes, cell lines and patient clinical data, to explore the succinate/SUCNR1 axis in hepatocytes in the context of NAFLD. We found that hepatocyte expression of *Sucnr1* is elevated in a murine model of diet-induced NASH and that hepatic SUCNR1 expression is an independent factor associated with NASH in patients. Mice lacking *Sucnr1* displayed both beneficial (reduced fibrosis and endoplasmic reticulum (ER) stress) and harmful (exacerbated steatosis and inflammation, and decreased glycogen content) features in the liver in response to NASH, with the latter reflected by systemic metabolic disturbances, particularly glucose intolerance. Results in hepatocytes supported a role for the succinate/SUCNR1 axis in modulating glycogen and lipid metabolism. Finally, analysis of clinical data of patients at risk of NAFLD identified succinate as a non-invasive biomarker for fatty liver diagnosis. Overall, our findings strengthen the idea of cell-specific effects of SUCNR1 and suggest the use of hepatocyte- or HSC-directed pharmacology with nanotechnology-based drug delivery systems [24] over strategies with agonists or antagonists of SUCNR1 to manage NAFLD.

2. Materials and methods

2.1. Human studies

We used four well-characterized cohorts: three of patients with obesity and one of a general population at risk of NAFLD. All participants provided written informed consent. The study was reviewed and approved by the Ethics and Research Committee of the corresponding institutions, according to Good Clinical Practice Guidelines of the Health Department of Generalitat de Catalunya, and met all requirements of the Declarations of Helsinki and Istanbul.

2.1.1. Subjects with obesity

Samples were used from patients with obesity with different degrees of steatosis undergoing bariatric surgery. Patients were recruited in three Spanish centers (Cohort I: Hospital Sant Joan de Reus, Reus; Cohort II: Hospital Virgen de la Arrixaca, Murcia; Cohort III: Hospital Josep Trueta, Girona). The local ethics committees approved the study (ESO3/18012013, #2020-2-4-HCUVA, 2009046, respectively) and all patients provided written informed consent. Exclusion criteria included history of cardiovascular disease, chronic inflammatory disease, liver disease other than NAFLD (hepatitis C or B, autoimmune liver disease, hemochromatosis), alcohol consumption >20 g/day, treatment with steatosis-inducing drugs and pharmacological anti-obesity treatments. In patients with T2D, antihyperglycemic medications were considered as confounding variables. Liver biopsies were classified by a pathologist according to the criteria of Brunt [25]: the severity of steatosis was graded from 0 to 3, inflammation from 0 to 3, hepatocellular ballooning from none to many, and fibrosis from 0 to 4. Based on these criteria, patients were included in the group of steatosis/fibrosis when the corresponding score was ≥1. Each liver specimen was assessed for the presence or absence of NASH by pattern recognition and NAFLD activity score (NAS), defined as the sum of steatosis, inflammation, and hepatocyte ballooning. Patients with NAS <3 were diagnosed as "not NASH", patients with 3 ≤ NAS < 5 as borderline and patients with NAS ≥ 5 as NASH [26]. Clinical and laboratory data are shown in Table 1.

2.1.2. Patients at risk of NAFLD

Patients for the NAFLD study were recruited in the setting of a multidisciplinary hepatology outpatient monographic clinic at the Joan XXIII University Hospital (Tarragona, Spain). The study was reviewed and approved by the Ethics and Research Committee of Institut d'Investigació Sanitària Pere Virgili (IISPV CEIm, Tarragona, Spain) (151/2019). In total, 101 patients with a wide range of body mass index (BMI) (21–43 kg/m^2) were included (Table 2). Patients were referred from general practitioners for diagnostic evaluation of NAFLD including

Table 1
Clinical and laboratory data of obese cohorts.

Obese cohorts	Cohort I ($n = 44$)	Cohort II ($n = 56$)	Cohort III ($n = 30$)
Sex, n (%)			
Females	32 (72.7)	40 (71.4)	22 (73.3)
Males	12 (27.3)	16 (28.6)	8 (26.7)
Age (years)	49.3 ± 10.0	47.5 ± 11.1	45.5 ± 8.4
BMI (kg/m^2)	47.1 ± 5.7	43.5 ± 6.0	44.7 ± 7.6
Waist circumference (cm)	133.7 ± 15.3	125.8 ± 14.0	124.2 ± 14.5
Systolic blood pressure (mm Hg)	138.9 ± 20.8	139.5 ± 21.4	139.5 ± 17.6
Diastolic blood pressure (mm Hg)	82.2 ± 26.8	82.8 ± 10.3	78.4 ± 14.5
Glucose (mg/dl)	147.2 ± 41.4	105.4 ± 44.3	108.9 ± 45.1
Insulin (μU/ml)	16.7 ± 12.6	16.4 ± 13.7	
HOMA-IR	6.5 ± 5.7	4.3 ± 4.0	4.0 ± 2.6
Total cholesterol (mg/dl)	173.7 ± 42.5	165.4 ± 29.6	186.3 ± 28.3
HDL cholesterol (mg/dl)	35.6 ± 10.4	43.3 ± 11.8	45.5 ± 8.1
LDL cholesterol (mg/dl)	122.9 ± 40.2	86.8 ± 27.4	116.4 ± 27.7
Triglycerides (mg/dl)	162.7 ± 79.6	184.5 ± 89.3	121.9 ± 48.7
ALT (U/l)	38.4 ± 18.0	23.7 ± 13.8	
AST (U/l)	40.8 ± 18.6	20.9 ± 9.3	22.0 ± 10.4
GGT (U/l)	28.8 ± 26.4	23.0 ± 16.4	31.8 ± 28.0
T2D, n (%)	17 (38.6)	26 (46.4)	7 (23.3)
Hypertension, n (%)	28 (63.6)	33 (58.9)	12 (40)
Dyslipidemia, n (%)	16 (36.4)	49 (87.5)	9 (30)
Steatosis, n (%)	34 (77.3)	40 (71.4)	20 (66.7)
Inflammation, n (%)	41 (93.2)	11 (19.6)	
Ballooning, n (%)	14 (31.8)	30 (53.6)	1 (3.3)
NAS ≥3, n (%)	35 (79.5)	24 (42.9)	5 (16.7)
Fibrosis, n (%)	35 (79.5)	0 (0)	6 (20)

Quantitative data are presented as mean ± SD. Abbreviations: BMI, body mass index; HDL, high-density lipoprotein; LDL low-density lipoprotein; ALT, alanine aminotransferase; AST, aspartate aminotransferase; GGT, gamma glutamyl transferase; T2D, type 2 diabetes mellitus; NAS, non-alcoholic fatty liver disease activity score.

Table 2
Clinical and laboratory data of population at risk of NAFLD.

NAFLD risk cohort	Cohort IV ($n = 101$)
Sex, n (%)	
Females	43 (42.6)
Males	58 (57.4)
Age (years)	57.2 ± 10.1
BMI (kg/m^2)	30.9 ± 4.8
Waist circumference (cm)	105.2 ± 11.7
Glucose (mg/dl)	111.0 ± 32.3
Insulin (μU/ml)	20.2 ± 14.3
HOMA-IR	5.9 ± 5.3
Total cholesterol (mg/dl)	198.3 ± 42.2
HDL cholesterol (mg/dl)	53.3 ± 15.3
LDL cholesterol (mg/dl)	113.3 ± 35.3
Triglycerides (mg/dl)	160.7 ± 88.8
ALT (U/l)	47.4 ± 33.2
AST (U/l)	34.4 ± 19.7
GGT (U/l)	86.7 ± 99.6
T2D, n (%)	28 (27.7)
Hypertension, n (%)	46 (45.5)
Dyslipidemia, n (%)	61 (60.4)
FLI	78.9 ± 18.4

Quantitative data are presented as mean ± SD. Abbreviations: BMI, body mass index; HDL, high-density lipoprotein; LDL low-density lipoprotein; ALT, alanine aminotransferase; AST, aspartate aminotransferase; GGT, gamma glutamyl transferase; T2D, type 2 diabetes mellitus; FLI, fatty liver index.

liver biopsy, when necessary, following the criteria of the hepatologist. Exclusion criteria included neoplastic or autoimmune disease, use of chemotherapy, immunosuppressors, immunomodulators, or corticoids, pregnancy, and alcohol consumption >30 g/day in men and 20 g/day in women. Patients were assessed for anthropometric, biochemical, and clinical measures after an overnight fast. Patients were classified according to the fatty liver index (FLI), an algorithm based on waist circumference, BMI, triglycerides (TG) and gamma-glutamyl transferase (GGT) (15 healthy patients and 86 patients with fatty liver). A subsample of 14 patients was classified according to hepatic steatosis grade at liver biopsy: 7 patients with no or a mild grade of hepatic steatosis (<33 % of hepatocytes with fat) and 7 patients with a moderate/severe grade (≥33 % of hepatocytes with fat).

2.2. Mice

Male C57BL/6J mice (wild-type, WT) were purchased from The Jackson Laboratory, and *Sucnr1*$^{-/-}$ mice on the same background were kindly provided by Dr. Kenneth McCreath (CNIC, Madrid, Spain). Mice were maintained at the Faculty of Medicine and Health Science animal facility of Rovira i Virgili University, and were housed 5 per cage under controlled conditions of 12-h light/dark at 22 °C with *ad libitum* access to diet and water. Mice were fed a choline-deficient high-fat diet (CD-HFD) (45 % fat, D05010402; Research Diets Inc.) for 15 weeks starting from 8 weeks of age. Body weight and food intake were recorded weekly. Mice were anesthetized with isoflurane and blood samples were obtained at sacrifice by cardiac puncture. All animal studies were supervised and approved by the Universitat Rovira i Virgili Animal Welfare and Governmental Ethics Committee (reference 10970). All experimental procedures involving animals conformed to the European Union Directive 2010/63/EU and the European Commission Recommendation 2007/526/EC on the protection of animals used for experimental and other scientific purposes, enacted under the Spanish Royal Decrees 53/2013 and 118/2021.

2.3. Cell cultures and treatments

2.3.1. Human primary hepatocytes

Human hepatocytes isolated from healthy human liver were provided by Innoprot and cultured following the instructions of the provider. Cells were treated with 0.2 mM palmitic acid (PA) or a vehicle for 24 h to study *SUCNR1* expression.

2.3.2. Human HepG2 cells

Human liver cancer HepG2 cells were obtained from the American Type Culture Collection, and were cultured in a humidified 5 % CO_2 incubator at 37 °C with DMEM/F12 medium (Cultek) supplemented with 10 % fetal bovine serum (FBS) (Sigma-Aldrich), 1 % penicillin-streptomycin (Cultek), 2 mM glutamine (PAN Biotech) and 20 mM Hepes (Cultek). Cells were cultured with FBS-free medium including 0.2 % bovine serum albumin (BSA) for 2–5 h prior to the experiment until its end. Cells were treated with PA, the SUCNR1 agonist cis-epoxysuccinic acid (cESA) [27] (TCI, Tokyo Chemical Industry), and the SUCNR1 antagonist NF56-EJ40 (MedChemExpress) [28]. Independent experiments (n) were conducted from different passages.

2.3.3. Isolation and culture of murine primary hepatocytes

Twelve-week-old mice and 8-week-old mice fed chow diet (CHD), HFD (60 % fat, D12492; Research diets) or CD-HFD for 16 weeks were used. Primary hepatocytes were isolated by liver perfusion with collagenase type IV from *Clostridium histolyticum* (Sigma-Aldrich) through the inferior cava vein [29,30]. Primary hepatocytes were used for gene expression analysis or were subjected to treatments. Cells from different mice were used as biological replicates (n).

2.4. Statistics

Significant differences between two groups were determined using unpaired or paired *t*-tests (two-tailed, 95 % confidence interval) when comparing the same group at different time points. For non-normal distributions, the Mann-Whitney test was employed. One-way ANOVA plus Tukey's multiple comparisons test was used to analyze the

differences between more than two groups. Two-way ANOVA was used to test statistical significance in the glucose (GTT) and insulin (ITT) tolerance tests. For clinical data, associations between quantitative variables were evaluated using Spearman correlation analysis. Regression analyses (stepwise forward selection procedures) and receiver operating characteristic (ROC) curves were employed to identify the prediction value of hepatic SUCNR1 or circulating succinate as independent factors related to NAFLD. Subsequently, the equality between the different ROC curve areas was tested. For categorical variables, the Chi-square test was used to determine significant differences between 3 groups, and Fisher's exact test was used to study differences between 2 groups. Scatter dot plots and time-course graphs data are presented in graphs as mean + SEM. Quantitative data in tables are presented as mean ± SD. The results were considered significant at $P < 0.05$. Statistical analyses were performed using SPSS (version 28.0, SPSS Inc.) or GraphPad Prism software (version 8.0, GraphPad Inc.). Graphical representations were generated with GraphPad Prism 8 Software.

Additional method details are provided in the supplementary appendix, including supplementary methods, Tables S1 and S2.

3. Results

3.1. *Sucnr1* expression in hepatocytes is elevated in animal models of diet-induced NASH

To investigate the role of the succinate/SUCNR1 axis in NAFLD, we first comparatively evaluated the expression of plasma membrane succinate transporters in primary hepatocytes isolated from mouse models of diet-induced NAFL (mice fed HFD [31,32]), NASH (mice fed CD-HFD [33–35]) (Table S3), and from control mice (fed CHD). The gene expression of succinate transporters was lower under HFD conditions than under CHD conditions (Fig. 1A). Importantly, both uptake (*Slc13a3* and *Slc13a5*) and release (*Slc22a7* and *Slc22a13*) succinate-transport systems were significantly upregulated in response to diet-induced NASH (Fig. 1A), indicating that succinate might function as a hepatocyte-derived paracrine signal for liver damage [36]. We also confirmed *Sucnr1* expression in the liver, albeit at lower levels than in adipose tissue (Fig. 1B), which agrees with previous reports [37]. As expected [17], both diet-induced NAFL and NASH triggered elevated *Sucnr1* expression in liver (Fig. 1C), which was also confirmed at the protein level in the NASH model (Fig. 1D). We also observed that *Sucnr1* expression in isolated hepatocytes was significantly higher in both diet models than in CHD conditions, particularly in the NASH model (Fig. 1E). Overall, the data suggest that the succinate/SUCNR1 axis might have signaling functions in hepatocytes beyond its role in HSC activation and fibrosis.

3.2. Elevated hepatic SUCNR1 expression is an independent factor of NASH

While there is some data on the circulatory pattern of succinate in the context of NAFLD in patients [8,9], only scarce information is available on liver SUCNR1 expression, which has been obtained from few subjects [22]. Single-cell RNA transcriptome landscaping of human liver recently identified *SUCNR1* expression in hepatocytes (among the 10 most expressed cell populations) but not in quiescent HSCs [38]. In agreement with the murine data, we found that *SUCNR1* expression was significantly higher in human primary hepatocytes (1.6-fold) and HepG2 cells (3.6-fold) treated with PA (a widely used *in vitro* challenge to mimic NAFLD) than in equivalent vehicle-treated cells (Fig. S1A, B). We assessed hepatic *SUCNR1* expression in liver biopsies of patients with obesity from three independent cohorts (clinical and anthropometrical characteristics summarized in Table 1). No statistically significant differences were found in hepatic *SUCNR1* expression in any cohort when classifying the data according to steatosis (Fig. 2A). However, hepatic *SUCNR1* expression was significantly higher in those patients classified with borderline/NASH according to the NAS (NAS ≥ 3) in Cohorts I and II (Fig. 2B). Strikingly, linear regression analysis revealed hepatic *SUCNR1* expression as a main determinant of NASH in persons with obesity and NAFLD after controlling for BMI, T2D, dyslipidemia and high blood pressure, in both cohorts (Table 3). We therefore pooled data from Cohort I and II and constructed a ROC curve to determine the

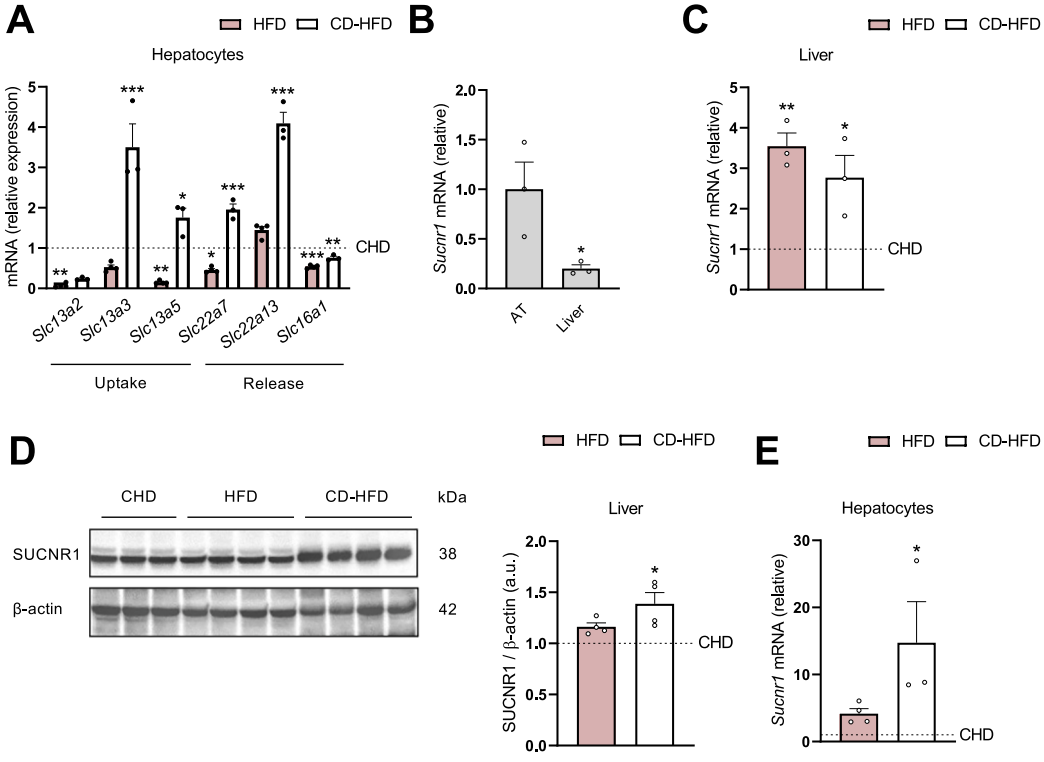

Fig. 1. Hepatic upregulation of succinate transporters and SUCNR1 in the context of NAFLD. Male C57BL6/J mice were fed a chow diet (CHD), high-fat diet (HFD) or a choline-deficient high-fat diet (CD-HFD) for 16 weeks. (A) RT-qPCR analysis of *Slc13a2*, *Slc13a3*, *Slc13a5*, *Slc22a7*, *Slc22a13* and *Slc16a1* in isolated hepatocytes (n = 3–4). (B) RT-qPCR analysis of *Sucnr1* in adipose tissue (AT) and liver from mice fed CHD (n = 3). (C) RT-qPCR analysis of *Sucnr1* in livers (n = 3–4). (D) Western blot analysis of SUNCR1 in livers (left panel) and densitometry analysis (right panel) (n = 3–4). (E) RT-qPCR analysis of *Sucnr1* in isolated hepatocytes (n = 3–4). All data are presented as mean + SEM and relative to CHD (dashed line). For (A, B, C) and (E), *B2m* expression was used to normalize data. For (D), β-actin was used as a loading control. Statistical significance between three groups was studied by one-way ANOVA, and an unpaired *t*-test was used for two groups; *$p < 0.05$; **$p < 0.01$; ***$p < 0.001$.

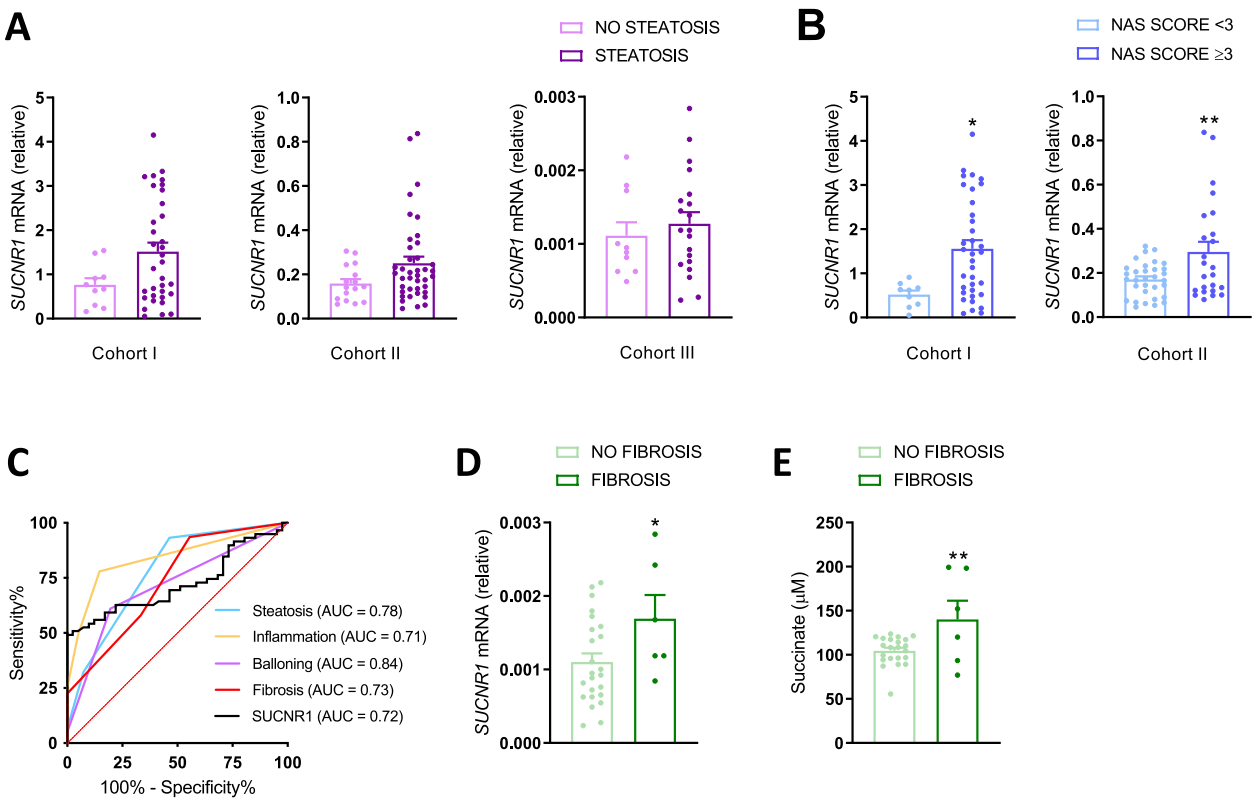

Fig. 2. Hepatic *SUCNR1* expression is elevated in human NASH and fibrosis. (A) Hepatic *SUCNR1* expression was analyzed by RT-qPCR according to steatosis in three independent cohorts. (B) In cohorts I (n = 44) and II (n = 56), hepatic *SUCNR1* expression was analyzed in patients classified by NAS. (C) In Cohort I and II, receiver operating characteristic curves were constructed for steatosis, ballooning, inflammation, fibrosis and SUCNR1 for predicting NASH risk. (D) In cohort III (n = 30), *SUCNR1* expression in liver from patients with or without fibrosis was determined by RT-qPCR. (E) Succinate was measured by a fluorimetric assay in blood samples from patients in Cohort III classified according to fibrosis. All results are expressed as mean + SEM, and, for gene expression, normalized to *18S* expression (A, B, D); $*p < 0.05$; $**p < 0.01$ (two-tailed unpaired *t*-test).

Table 3
Linear regression model for the prediction of NAS ≥3 in Cohort I and Cohort II.

Cohort I	NAS ≥ 3 ($R = 0.384$; $R^2 = 0.147$)				
Variable	β (Non-standardized)	SE	95 % CI	β (Standardized)	*P*-value
Constant	0.605	0.091	0.421–0.789	–	<0.001
SUCNR1	0.141	0.053	0.036–0.247	0.384	0.010

Cohort II	NAS ≥ 3 ($R = 0.370$; $R^2 = 0.137$)				
Variable	β (Non-standardized)	SE	95 % CI	β (Standardized)	P-value
Constant	0.183	0.105	−0.027-0.393	–	0.086
SUCNR1	1.095	0.374	0.344–1.845	0.370	0.005

Variables included in the regression model were *SUCNR1*, body mass index, type 2 diabetes, dyslipidemia and high blood pressure. Abbreviations: NAS, non-alcoholic fatty liver disease activity score; SUCNR1, succinate receptor 1.

predictive capacity of hepatic *SUCNR1* expression for developing NASH. Results showed that *SUCNR1* expression had a similar sensitivity and specificity to that of steatosis, inflammation and fibrosis (AUC = 0.72) (Fig. 2C). These results were not found for Cohort III (Fig. S2A), likely due to the reduced number of subjects, and to differences in lipid profiles (Table S4) and the percentage of ballooning, NAS ≥ 3 and fibrosis compared with the other cohorts (Table S5). Of note, we observed an upregulation of *SUCNR1* in patients with fibrosis in Cohort III (Fig. 2D), which was concomitant with higher levels of circulating succinate (Fig. 2E). These differences were not observed in Cohort I (Fig. S2B, C), presumably because of the variability in clinical and anthropometrical data (Tables S4, 5). Altogether, the patient data reflect the heterogeneity of the disease [39] and point to the involvement of SUCNR1 in NAFLD progression to more advanced stages.

3.3. *Sucnr1* deficiency impacts the systemic and liver phenotype of mice with diet-induced NASH

To study the relevance of the succinate/SUCNR1 axis in NAFLD development *in vivo*, we explored the response of global *Sucnr1*$^{-/-}$ mice to diet-induced NASH. *Sucnr1*$^{-/-}$ and WT mice had a similar body weight before and 15 weeks after the CD-HFD intervention (Fig. 3A). Unexpectedly, however, when compared with WT mice, *Sucnr1*$^{-/-}$ mice showed an increase in fasting blood glucose concentrations (Fig. 3B) and impaired glucose tolerance (Fig. 3C). Deficiency of *Sucnr1* had no effect on insulin secretion (Fig. 3D), but whole-body insulin sensitivity (measured by an ITT) (Fig. 3E) and HOMA-IR and QUICKI indices (Fig. 3F) were impaired in *Sucnr1*$^{-/-}$ mice. Consistent with the reported pro-fibrogenic function of SUCNR1 in HSCs [17,18,40], the degree of hepatic fibrosis associated with CD-HFD was lower in *Sucnr1*$^{-/-}$ mice than in WT mice, as demonstrated by Collagen type I alpha 1 (*Col1a1*) gene expression (Fig. 3G), α-smooth actin (α-SMA) protein expression (Fig. 3H) and Masson's trichrome staining of liver sections (Fig. 3I). Likewise, we noted a reduction in the expression of ER stress markers (the phosphorylated form of alpha subunit of eukaryotic initiation factor 2, p-eiF2α, and C/EBP-homologous protein, CHOP), which are well known pro-fibrotic stimuli [41], in liver biopsies of *Sucnr1*$^{-/-}$ mice (Fig. 3J). Contrastingly, hepatic steatosis was more severe in *Sucnr1*$^{-/-}$ mice than in WT mice in response to the NASH challenge (Fig. 3K, L),

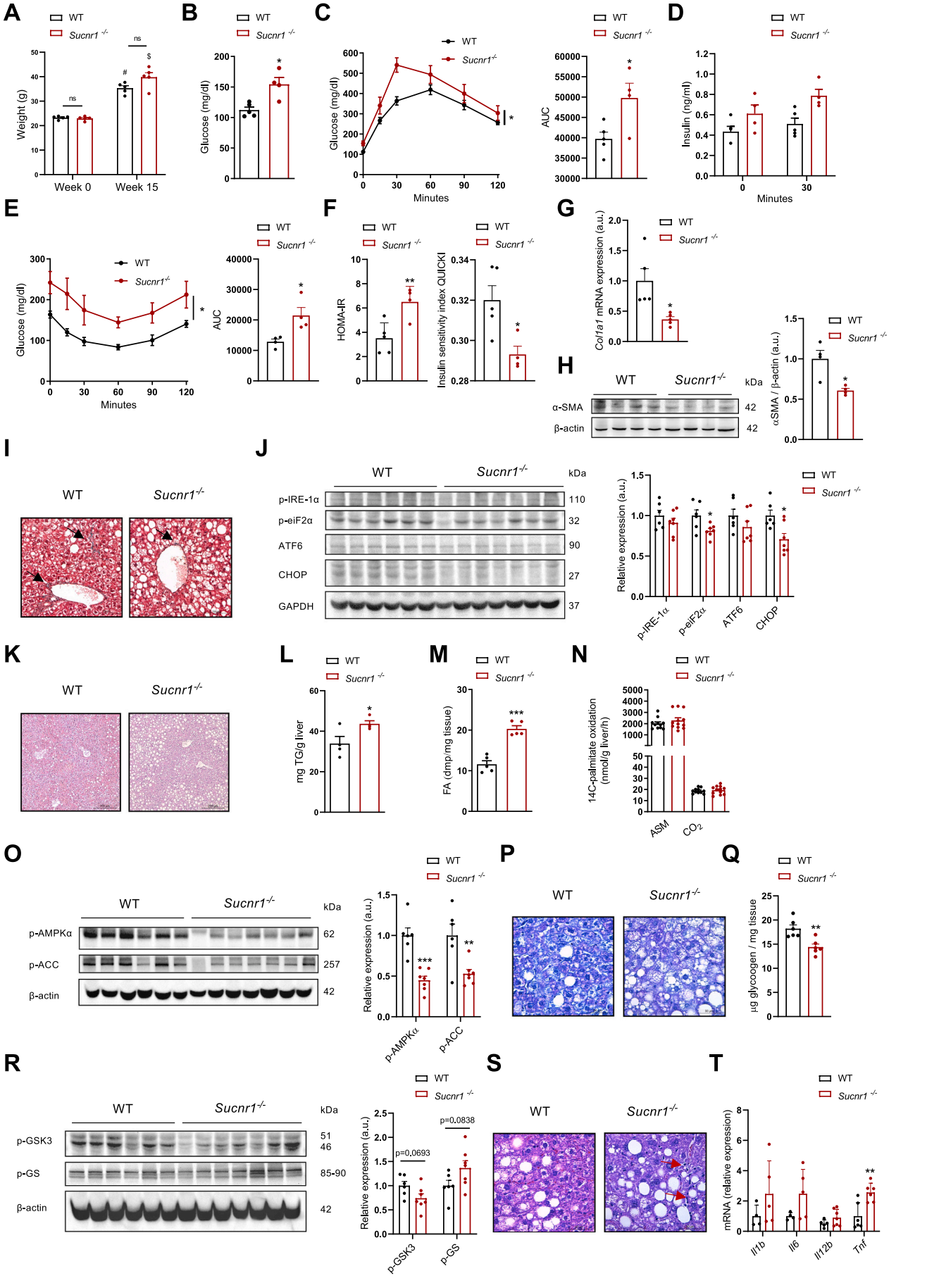

(caption on next page)

Fig. 3. Systemic and liver alterations in *Sucnr1*$^{-/-}$ mice with diet-induced NASH. Eight-week-old wild-type (WT) and *Sucnr1*$^{-/-}$ mice were fed a choline-deficient high-fat diet (CD-HFD) for 15 weeks to induce NASH. (A) Initial and final body weights. (B) Fasting glucose concentrations in blood. (C) Glucose tolerance test (GTT) and its respective AUC. (D) Insulin concentration in blood (basal and 30 min after of glucose injection). (E) Insulin tolerance test (ITT) and its respective AUC. (F) HOMA-IR (left) and QUICKI (right). (G) RT-qPCR analysis of *Col1a1* mRNA expression in liver. (H) Western blotting of α-smooth actin in liver, with densitometry analysis. (I) Masson's trichrome staining (×24) of liver sections; black arrows indicate collagen. (J) Western blotting of endoplasmic reticulum stress markers in the liver (left panel) and their respective densitometry analysis (right panel). (K) Hematoxylin and eosin staining of liver sections (×10). (L) Triglycerides (TG) content in the liver. (M) *De novo* lipogenesis of fatty acids (FAs) in liver tissue. (N) Rate of FA oxidation in liver tissue determined by the production of acid-soluble metabolites (ASM) and CO_2. (O) Western blotting of phospho-AMPKα and phospho-acetyl-CoA carboxylase in liver samples (left panel) and densitometry analysis (right panel). (P) Periodic acid-Schiff staining of glycogen accumulation (×40) in liver. (Q) Glycogen quantification in liver. (R) Western blotting of proteins involved in glycogen metabolism in liver (left panel) and densitometry analysis (right panel). (S) Hematoxylin and eosin staining of liver tissue; red arrows indicate immune cells (×40). (T) RT-qPCR analysis of pro-inflammatory cytokine genes in liver. All data is presented as mean + SEM and normalized to WT values (n = 4–7). For protein blots, data were normalized to β-actin (H, O, R) or GAPDH (J) expression. For RT-qPCR analysis (G, T), data were normalized to *B2m* expression. For bar graphs, statistical significance between genotypes was calculated with a two-tailed unpaired *t*-test, and differences between time points in the same group were analyzed with a two-tailed paired *t*-test. For GTT and ITT curves, two-way ANOVA was used. $^{\#}p < 0.001$ *versus* WT mice at week 0; $^{\$}p < 0.001$ *versus Sucnr1*$^{-/-}$ mice at week 0; $^{*}p < 0.05$ *versus* WT; $^{**}p < 0.01$ *versus* WT; $^{***}p < 0.001$ *versus* WT; ns, non-significant. (For interpretation of the references to color in this figure legend, the reader is referred to the web version of this article.)

which was accompanied by an increase in *de novo* fatty acid synthesis (Fig. 3M) without substantial changes in fatty acid oxidation rates (Fig. 3N). Furthermore, the level of phosphorylation of 5′ AMP-activated protein kinase α (AMPKα) and acetyl-CoA carboxylase (ACC) (Fig. 3O), a key pathway that inhibits lipid synthesis [42], was significantly lower in *Sucnr1*$^{-/-}$ mice than in WT mice. Considering the anti-lipolytic role of SUCNR1 in adipose tissue [15], we evaluated whether the steatosis in *Sucnr1*$^{-/-}$ mice was associated with the increased delivery of free fatty acids (FFAs) to the liver. Indeed, we found elevated FFAs in circulation (Fig. S3A) and reduced adipocyte area in subcutaneous white adipose tissue (Fig. S3B) but not in visceral white adipose tissue (Fig. S3C). Moreover, liver glycogen content was significantly lower in *Sucnr1*$^{-/-}$ mice than in WT mice (Fig. 3P, Q), which correlated with an inhibition of the glycogenesis pathway in *Sucnr1*$^{-/-}$ mice as indicated by the reduced levels of phospho-glycogen synthase kinase 3 α/β (p-GSK3α/β) (inactive form of GSK3) and higher levels of the inactive form of glycogen synthase (p-GS) (Fig. 3R). Consistent with the elevated lipid deposition in liver, immune cell infiltration (foci) was greater in the liver of *Sucnr1*$^{-/-}$ mice than in WT mice, as observed by H&E staining (Fig. 3S) and by the expression of pro-inflammatory cytokines, reaching significance for Tumor necrosis factor alpha (*Tnf*) (Fig. 3T).

Overall, the results indicate that SUCNR1 signaling might have pleiotropic effects on the hepatic metabolic changes occurring during NAFLD progression, including the negative regulation of lipogenesis and the positive regulation of glycogenesis.

3.4. SUCNR1 activation protects hepatocytes from lipid accumulation and glycogen depletion induced by NAFLD challenge

We next performed *in vitro* experiments to directly test whether the metabolic changes observed *in vivo* are a consequence of the loss of SUCNR1 signaling in hepatocytes, rather than a reflection of its impact on HSCs and fibrosis. We established cultures of primary murine hepatocytes treated with PA to induce lipid storage and lipotoxicity. In WT hepatocytes, PA treatment triggered lipid deposition, as shown by an increase in Oil Red O staining, and this was significantly attenuated in cells co-treated with the SUCNR1 agonist cESA (Fig. 4A). Likewise, there was a trend for a decrease in lipid content and in the expression of key genetic regulators of lipogenesis in PA-treated HepG2 cells co-treated with cESA (Fig. S2A, B). In contrast to its effects on WT cells, cESA co-treatment had no effect on lipid accumulation in PA-treated *Sucnr1*$^{-/-}$ primary hepatocytes (Fig. 4B). Co-treatment of PA-treated primary murine WT hepatocytes with cESA induced the phosphorylation and activation of AMPKα, a key regulator of fatty acid metabolism (Fig. 4C), and also stimulated the phosphorylation of protein kinase A subunit C (PKA-C) and the downstream signaling protein CREB (Fig. 4C), which has been reported as an inhibitor of the transcription of lipogenic genes [43].

We next studied the modulation of glycogen metabolism through SUCNR1. As previously reported [44], PA treatment reduced the glycogen accumulation both in WT and *Sucnr1*$^{-/-}$ primary hepatocytes, as revealed by immunofluorescence staining with an anti-glycogen antibody (Fig. 4D). Of note, we observed fewer glycogen granules in primary *Sucnr1*$^{-/-}$ hepatocytes both with vehicle and PA treatments (Fig. 4D), which for the latter is in accordance with the *in vivo* analysis of mice on CD-HFD (Fig. 3P, Q). Short-term treatment with cESA promoted GSK3α/β phosphorylation (inactive form) and GS dephosphorylation (active form) in primary murine WT hepatocytes treated with PA (Fig. 4E), suggesting an increase in glycogen synthesis. Notably, glycogen synthesis through succinate and cESA was reproduced in PA-treated human HepG2 cells, as demonstrated by glycogen quantification (Fig. S2C) and GS dephosphorylation (Fig. S2D). These findings indicate that SUCNR1 signaling promotes the restoration of glycogen accumulation in hepatocytes under lipotoxic conditions. Finally, given that hepatocytes secrete elevated amounts of succinate to the extracellular space under lipotoxicity [17], we sought to confirm an autocrine/paracrine function of succinate in hepatocytes. Of note, PA-treated HepG2 cells further stimulated with a SUCNR1 antagonist showed lower glycogen levels than non-stimulated cells (Fig. 4F), suggesting that hepatocyte-derived succinate might have autocrine and paracrine effects on glycogen metabolism through SUCNR1.

Altogether, our findings show that while blocking SUCNR1 might improve fibrosis, it also exacerbates disturbances in NAFLD-related lipogenesis and glucose metabolism.

3.5. Circulating succinate is an early biomarker of steatosis in population at risk of NAFLD

The prevalence of NAFLD in the general population has been estimated to be ~25 % [45]; however, this might be an underestimation given the nonspecificity of symptoms and the lack of reliable non-invasive biomarkers for diagnosis. The FLI is an accurate and simple algorithm to employ in routine clinical practice to identify subjects at high risk of developing fatty liver disease [46]. In a fourth cohort of 93 subjects with a wide BMI range classified according to FLI (patients at risk, Table 2), we observed that circulating succinate levels were elevated in subjects with a high FLI (≥60, indicative of hepatic steatosis), with a positive correlation between circulating succinate and the FLI scale (Fig. 5A, B). To determine the value of circulating succinate levels in predicting hepatic steatosis in a population at risk of NAFLD, we generated an ROC curve that included all of the components of FLI plus succinate levels. Of note, circulating succinate had a good predictive capacity (AUC = 0.77, 95 % CI 0.66–0.87), which was slightly lower than the anthropometric variables and greater than the analytical measures (GGT and TG) (Fig. 5C). To further confirm the potential role of circulating succinate to predict early stages of fatty liver and as a method to prevent unnecessary liver biopsies or to improve the indication of their need, 14 patients of this cohort with available liver samples

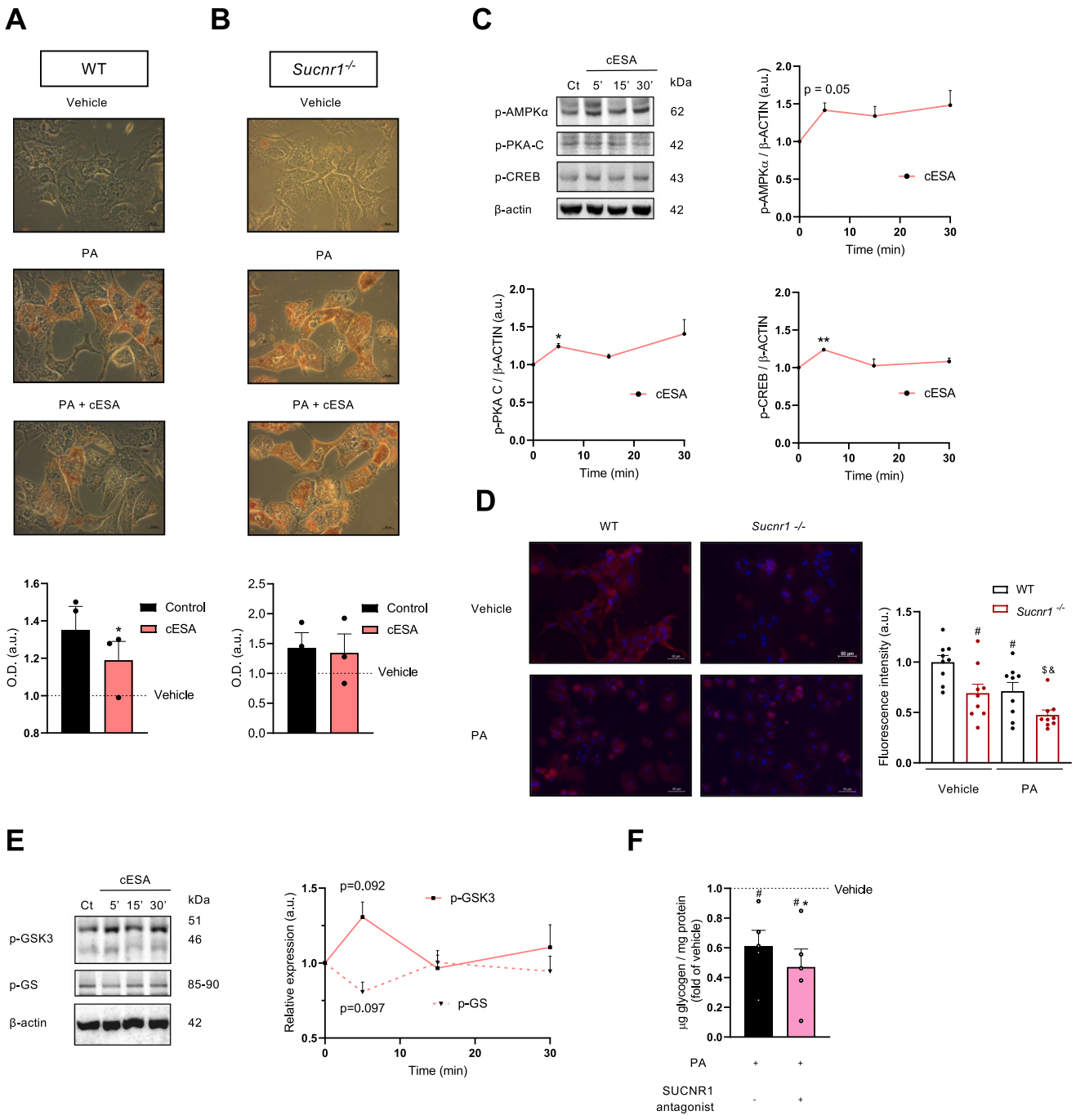

Fig. 4. SUCNR1 governs lipid and glycogen content in murine primary hepatocytes in NAFLD. (A-B) Oil red O staining of deposited lipids (upper panel) and relative quantification with 2-propanol (lower panel) in primary murine hepatocytes isolated from (A) WT or (B) *Sucnr1*$^{-/-}$ mice previously treated with PA or vehicle and then stimulated with cESA for 24 h (n = 3). (C) Western blotting and densitometry analysis of p-AMPKα (upper panel), p-PKA-C and p-CREB (lower panel) in response to cESA stimulation (100 µM) in primary murine hepatocytes isolated from WT mice and treated with PA for 27 h (n = 3). (D) Glycogen immunofluorescence in vehicle- and PA-treated hepatocytes isolated from WT and *Sucnr1*$^{-/-}$ mice (left panel) and relative quantification with ImageJ (right panel) (*n* = 3, 3 images from each mouse). (E) Western blotting of p-GSK3 α/β and p-GS and densitometry analysis in response to cESA stimulation (100 µM) of primary hepatocytes isolated from WT mice and treated with PA for 27 h (n = 3). (F) Glycogen quantification in human HepG2 cells in response to treatment of PA or PA plus a SUCNR1 antagonist (1 µM) compared with vehicle (n = 5). Data are presented as mean + SEM and normalized to the vehicle values (A, B, F), no cESA treatment (C, E) or WT vehicle (D). For protein blots, data were normalized to β-actin (C, E). *p < 0.05 *vs* control PA; **p < 0.01 *vs* control PA (two-tailed paired *t*-test). $^{\#}$p < 0.05 *vs* Vehicle WT; $^{\$}$p < 0.05 *vs* vehicle *Sucnr1*$^{-/-}$; $^{\&}$p < 0.05 *vs* PA WT (two-tailed unpaired *t*-test). (For interpretation of the references to color in this figure legend, the reader is referred to the web version of this article.)

were classified according to the grade of hepatic steatosis diagnosed by biopsy (7 patients with no or mild steatosis and 7 patients with moderate or severe steatosis). ROC curves were then constructed to assess the performance of FLI, succinate, and a model including FLI and succinate (FLISucc). Notably, circulating succinate had a similar AUC (0.69, 95 % CI 0.4–0.98) to FLI (0.63, 95 % CI 0.32–0.94) and the FLISucc model exhibited an improved predictive capacity (AUC = 0.78, 95 % CI 0.52–1.0), albeit without reaching significance (Fig. 5D). Although further studies will be required, the present findings allow us to speculate that circulating succinate, an excellent marker of metabolic status,

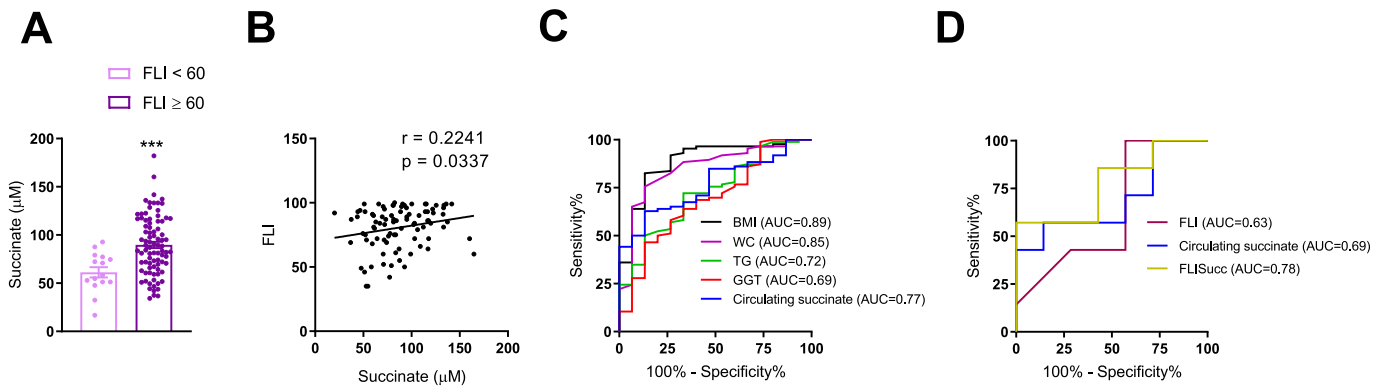

Fig. 5. Circulating succinate is a non-invasive biomarker of fatty liver in a population at risk of NAFLD. (A) Circulating succinate measured by fluorometric assay in patients classified according to fatty liver index (FLI). (B) Spearman's correlation between FLI and circulating succinate. (C) ROC curves for body mass index (BMI), waist circumference (WC), triglycerides (TG), gamma-glutamyl transferase (GGT) and succinate in predicting fatty liver. (D) ROC curves for FLI, circulating succinate and the combination of FLI plus succinate (FLISucc) in predicting moderate/severe steatosis through biopsy in a subset of patients from cohort IV. For (A, B, C), n = 101 and for (D), $n = 14$. Results are expressed as mean + SEM; ***p < 0.001 (two-tailed unpaired *t*-test).

might have potential as a non-invasive biomarker for early stages of fatty liver disease.

4. Discussion

Our study identifies SUCNR1 as an autocrine/paracrine sensor of hepatocyte damage with a likely key function in NAFLD. Beyond its described role in fibrosis [17,18,20–22,36,40], we show that the succinate/SUCNR1 axis behaves as a counteracting effector of NAFLD-induced steatosis, inflammation and aberrant glycogen metabolism. We also provide meaningful clinical data for hepatic *SUCNR1* expression as a diagnostic hallmark of NASH, and for circulating succinate as a non-invasive biomarker of fatty liver in a population at risk of NAFLD. Overall, our findings point to the succinate/SUCNR1 axis as an important regulator of liver disease progression in a cell-dependent manner.

In the context of obesity, although there were disparities between some cohorts, SUCNR1 was overexpressed in liver from patients with NAS ≥ 3 and fibrosis, making it a good determinant of NAFL progression to NASH and fibrosis in this population. These findings are in accordance with previous results of SUCNR1 immunohistochemistry in liver biopsies from a small cohort of patients graded by NAS and fibrosis [22]. We also confirmed that Sucnr1 is elevated in liver from mice with diet-induced NASH, as described [17], although its downregulation has also been reported [47]. These contentious findings might be explained by the differences in diet composition and duration. Focusing on hepatocytes, we found that the expression of succinate transporters was oppositely regulated by NAFL compared with NASH. Further studies are warranted to discern whether this contrasting regulation might be a consequence of the absence of choline in the diet used to induce NASH, or whether it indicates that succinate transport is differentially regulated depending on the NAFLD stage. In the latter case, the underlying mechanism may include SUCNR1 expression and activation, as described for renal cells [48]. Of note, the upregulation of succinate transport systems in NASH is consistent with a study describing succinate as a key player in the crosstalk between hepatocytes and activated HSCs through SUCNR1 [17]. Importantly, we also describe for the first time an upregulation of *Sucnr1* in hepatocytes from NASH-challenged mice, which was also observed in diet-induced obese mice, although no statistical significance was reached. This suggests that SUCNR1 signaling in hepatocytes is relevant under conditions of NASH, which provides new insight into SUCNR1 in liver disease. Indeed, single-cell RNA analysis revealed *SUCNR1* expression in human hepatocytes [38], highlighting the likely importance of the receptor in this cell type.

Although tissue/cell-selective knockout models are the best tools to study the cell-intrinsic functions of genes, NAFLD is characterized by complex intercellular and interorgan crosstalk [49] and, accordingly, the global *Sucnr1* knockout model used here can capture the prominent features of loss of the receptor. As expected, we found that *Sucnr1* deficiency ameliorated liver fibrosis [17,18,40] and ER stress [50]; however, rather than yielding a better metabolic profile, it exacerbated the disturbances in glucose homeostasis induced by NASH. Of particular note was the increase in hepatic lipid accumulation induced by diet-induced NASH in *Sucnr1*$^{-/-}$ mice, which contrasts with an earlier study using a methionine- and choline-deficient diet [17]. The latter diet results in a rapid NASH phenotype but also induces weight loss, which would suggest that the modulation of hepatic steatosis by SUCNR1 is also dependent on the metabolic phenotype. Indeed, our data on adipose tissue morphology and FFAs suggest that the hepatic steatosis might be, at least in part, a reflection of unrestrained lipolysis in adipose tissue due to the lack of *Sucnr1* and subsequent exacerbated transport of FFAs to liver, which has been intensely investigated with different experimental approaches [15,51–53]. Nevertheless, we also found a significant increase in *de novo* lipogenesis in liver, indicating that *Sucnr1* deficiency in both organs might contribute to the evident hepatic steatosis. Remarkably, our data also revealed that hepatic glycogen content is influenced by *Sucnr1* deficiency. It is well known that hepatic glycogen falls once insulin resistance is established due to reduced glycogen synthesis and increased glycogen degradation [42]. In agreement with the reduced insulin sensitivity, global *Sucnr1* deficiency also led to a reduction of glycogen levels in liver in response to NASH challenge. Glycogen has been previously described as a trigger of lipogenesis in the context of nutrient excess [54], yet *Sucnr1* deficiency resulted in the uncoordinated synthesis of glycogen and lipids, which supports a broad role for SUCNR1 in hepatic metabolism. In parallel with the defective fat and glycogen metabolism in liver, *Sucnr1*$^{-/-}$ mice showed exacerbated inflammation. This agrees with our previous studies showing that myeloid-cell-specific *Sucnr1*-deficient mice have an overall pro-inflammatory phenotype [11], although these results contrast with the anti-inflammatory phenotype observed in Kupffer cells isolated from global *Sucnr1* knockout mice on chow diet [19], overall indicating that the phenotypic outcome depends on the metabolic background and the target cell. Our *in vivo* findings argue against the proposal of using SUCNR1 antagonists as a therapy for NASH [23], as global *Sucnr1* deficiency improves fibrosis but dysregulates hepatic metabolism and impairs glucose homeostasis.

While dysfunctional succinate/SUCNR1 signaling in adipose tissue might partially underlie the metabolic phenotype *in vivo*, our *in vitro* data identify hepatocytes as target cells of extracellular succinate, particularly in the context of NAFLD. Thus, our findings reveal a hitherto unrecognized role of SUCNR1 as a key regulator of the crosstalk between

lipid and glycogen metabolism in NASH-affected hepatocytes, which together with its role in adipocytes might contribute to the metabolic phenotype observed *in vivo*. SUCNR1 activation had no impact on lipogenesis or glycogenesis in HepG2 cells under basal conditions, likely due to its low gene and protein expression, but reversed the effects of NASH challenge (which upregulated the expression of the receptor) on glycogen content and fat accumulation in both human HepG2 cells and murine primary hepatocytes, in agreement with our findings in liver. Specifically, we found that the SUCNR1 agonist cESA regulates both lipogenic and glycogenic signaling including the PKA/CREB, AMPK and GSK3/GS pathways, explaining, at least in part, the mechanism of action of SUCNR1 in hepatocytes.

The above-described outcomes of succinate signaling in liver point to succinate as an alarmin secreted by damaged hepatocytes, similar to danger-associated molecular patterns such as hepatocyte mitochondria-derived danger signals [55,56] or IL-33 [57]. Interestingly, IL-33 was reported to ameliorate hepatic steatosis and promote an anti-inflammatory program in NASH liver, but also aggravated hepatic fibrosis [58], which is similar to our observations with succinate. Accordingly, succinate might be secreted in response to injury and act through SUCNR1 in different liver cells to activate tissue repair mechanisms, such as reprogramming lipid and glycogen metabolism in hepatocytes, modulating inflammatory processes in immune cells, and stimulating fibrosis in HSCs, although disproportionately in the latter case.

In the clinical setting, it is conceivable that circulating levels of succinate might reflect disease progression. We identified succinate as a potential early biomarker of hepatic steatosis (diagnosed both by FLI and liver biopsy) in a cohort of patients at risk of NAFLD, which is in accord with a smaller cohort study comparing patients with hepatic ultrasound-diagnosed NAFLD with healthy controls [8]. This association was not observed in obese cohorts, where the majority of patients were women. While it is well-established that sex can impact the prevalence, influencing factors, pathophysiology, complications and efficacy of therapies in NAFLD [59], our analysis did not reveal any significant differences in succinate levels or *SUCNR1* expression between sexes in any of the cohorts (data not shown). These findings suggest that sex may not significantly influence our results.

It is important to note that prospective long-term follow-up studies will be needed to confirm the utility of succinate as a clinical tool to identify patients at high risk of developing a more aggressive phenotype.

5. Conclusions

Our data support the idea that the succinate/SUCNR1 axis might play a crucial role in the progression of NAFLD to NASH. However, our data suggest a different concept for this pathway as merely an activator of fibrosis. Thus, succinate-SUCNR1 signaling is placed as a protective mechanism–likely activated at early stages–to counteract inflammation, lipid overload and glycogen depletion in damaged hepatocytes, at the expense of activating fibrosis, rather than as a driver of pathology *per se*. This is consistent with the notion of hepatocyte mitochondria-derived molecules as danger signals by triggering pro-fibrotic HSCs activation [58], with an excessive fibrotic response and disease progression ultimately the consequence of a failure of this protective mechanism. Our data thus strengthens the need for a cell-specific study of SUCNR1 function to develop future cell-directed pharmacology [24].

We acknowledge some limitations in our study. Our proposal of circulating succinate as a biomarker of fatty liver will need to be tested in a validation cohort of patients at risk of NAFLD from a different geographical location. Also, a murine model of hepatocyte-specific deletion of *Sucnr1* would be useful to determine the specific contribution of both liver and adipose tissue to the systemic phenotype.

Funding

This study was supported by grants from MCIN/AEI/10.13039/501100011033 (SAF2015-65019-R, RTI2018-093919-B-100 and PID2021-122480OB-100 to S.F.-V.; PID2021-122766OB-100 to A.M.V; PID2021-124425OB-I00 to P.A.) co-financed by the European Regional Development Fund (ERDF) and Grupos consolidados Gobierno Vasco IT1476-22 to P.A. This research was funded by the Institute of Health "Carlos III" (ISCIII) and co-financed by ERDF (PI20/00095 to V.C.-M.; PI20/00338 to J.V. and PI20/00505 to B.R.-M.). This study was also supported by a grant from ISCIII and CIBERDEM, DEM19PI01/2019 to V.C.-M. and P.R. The project that gave rise to these results received funding from "La Caixa" Foundation (ID 100010434), under the grant agreement LCF/PR/HR20/52400013 (to S.F.-V.). This study was also supported by Rovira i Virgili University and Tarragona Provincial Council with the Talent Salut fellowship to A.R.-C. A.M.-B. is a recipient of an FPU grant (FPU20/05633) from MCIN/AEI/10.13039/501100011033. B.A. acknowledges support from the PERIS program 2016–2020 (LT017/20/000033), from Departament de Salut de la Generalitat de Catalunya. V.C.-M. acknowledges support from the Ramón y Cajal program (RYC2019-02649-I), from MCIN/AEI/10.13039/501100011033/ and the European Social Fund (ESF), "Investing in your future". B.R.-M. acknowledges support from the Miguel Servet Type I program (CP19/00098) from the Fondo de Investigación Sanitaria, co-financed by the ERDF. SFV and JVO acknowledge support from the Agency for Management of University Research Grants of the Generalitat de Catalunya (2021 SGR 01409, 2021 SGR 0089). The study was also supported by CIBER–Consorcio Centro de Investigación Biomédica en Red (CB07708/0012), ISCIII, Ministerio de Ciencia e Innovación.

Data statement

The data that supports the findings of this study are available in the manuscript and in the supplementary appendix of this article.

CRediT authorship contribution statement

AM-B: Methodology, Validation, Formal analysis, Investigation, Writing – Original draft, Visualization. **AR-C**: Methodology, Investigation, Resources. **BA**: Methodology, Validation, Investigation. **EC**: Methodology, Validation, Formal analysis, Investigation. **PR**: Methodology, Validation, Investigation, Resources, Funding acquisition. **AM**, **M-MR-P**, **CN-R** and **EM-M**: Methodology, Validation, Investigation. **GL**: formal analysis, visualization. **BG-S**: Methodology, Resources. **RB**: Validation, Resources. **MDF**, **J-MM-N**, **BR-M**, **PA**, **JJ**, **J-MF-R**, **JCQ**, **AMV** and **AP**: Resources, Critical review. **JV**: Writing – Original draft, Funding acquisition. **VC-M**: Conceptualization, Validation, Formal analysis, Investigation, Writing – Original draft, Supervision, Funding acquisition. **SF-V**: Conceptualization, Validation, Writing – Original draft, Supervision, Project administration, Funding acquisition.

Declaration of competing interest

None.

Acknowledgements

Assistance with the study: We particularly acknowledge the patients, the BIOBANC-MUR (PT20/00109), the BioBank IISPV (PT17/0015/0029) and the BioBank IDIBGI (ICS.00258) integrated in the Spanish National Biobanks Network for its collaboration. We thank Dr. Kenneth McCreath for helpful comments on the manuscript. We also thank Dr. Otto Baba (Baba, 1993) for his generous gift of the monoclonal glycogen antibody.

Appendix A. Supplementary data

Supplementary data to this article can be found online at https://doi.org/10.1016/j.metabol.2023.155630.

References

[1] Younossi ZM, Marchesini G, Pinto-Cortez H, Petta S. Epidemiology of nonalcoholic fatty liver disease and nonalcoholic steatohepatitis: implications for liver transplantation. Transplantation 2019;103:22–7. https://doi.org/10.1097/TP.0000000000002484.

[2] Buzzetti E, Pinzani M, Tsochatzis EA. The multiple-hit pathogenesis of non-alcoholic fatty liver disease (NAFLD). Metabolism 2016;65:1038–48. https://doi.org/10.1016/j.metabol.2015.12.012.

[3] Ferguson D, Finck BN. Emerging therapeutic approaches for the treatment of NAFLD and type 2 diabetes mellitus. Nat Rev Endocrinol 2021;17:484–95. https://doi.org/10.1038/S41574-021-00507-Z.

[4] Chalasani N, Younossi Z, Lavine JE, Charlton M, Cusi K, Rinella M, et al. The diagnosis and management of nonalcoholic fatty liver disease: practice guidance from the American Association for the Study of Liver Diseases. Hepatology 2018;67:328–57. https://doi.org/10.1002/hep.29367.

[5] Serena C, Ceperuelo-Mallafré V, Keiran N, Queipo-Ortuño MI, Bernal R, Gomez-Huelgas R, et al. Elevated circulating levels of succinate in human obesity are linked to specific gut microbiota. ISME J 2018;12:1642–57. https://doi.org/10.1038/s41396-018-0068-2.

[6] Ceperuelo-Mallafre V, Llaurado G, Keiran N, Benaiges E, Astiarraga B, Martinez L, et al. Preoperative circulating succinate levels as a biomarker for diabetes remission after bariatric surgery. Diabetes Care 2019;42:1956–65. https://doi.org/10.2337/dc19-0114.

[7] Osuna-Prieto FJ, Martinez-Tellez B, Ortiz-Alvarez L, Di X, Jurado-Fasoli L, Xu H, et al. Elevated plasma succinate levels are linked to higher cardiovascular disease risk factors in young adults. Cardiovasc Diabetol 2021;20:151. https://doi.org/10.1186/s12933-021-01333-3.

[8] Chashmniam S, Ghafourpour M, Farimani AR, Gholami A, Ghoochani BFNM. Metabolomic biomarkers in the diagnosis of non-alcoholic fatty liver disease. Hepat. Mon. 2019;19:e92244. https://doi.org/10.5812/hepatmon.92244.

[9] Loomba R, Seguritan V, Li W, Long T, Klitgord N, Bhatt A, et al. Gut microbiome based metagenomic signature for non-invasive detection of advanced fibrosis in human nonalcoholic fatty liver disease. Cell Metab 2017;25:1054–62. https://doi.org/10.1016/j.cmet.2017.04.001.Gut.

[10] Fernández-Veledo S, Ceperuelo-Mallafré V, Vendrell J. Rethinking succinate: an unexpected hormone-like metabolite in energy homeostasis. Trends Endocrinol. Metab. 2021;32:680–92. https://doi.org/10.1016/J.TEM.2021.06.003.

[11] Keiran N, Ceperuelo-Mallafré V, Calvo E, Hernández-Alvarez MI, Ejarque M, Núñez-Roa C, et al. SUCNR1 controls an anti-inflammatory program in macrophages to regulate the metabolic response to obesity. Nat Immunol 2019;20:581–92. https://doi.org/10.1038/s41590-019-0372-7.

[12] Trauelsen M, Rexen Ulven E, Hjorth SA, Brvar M, Monaco C, Frimurer TM, et al. Receptor structure-based discovery of non-metabolite agonists for the succinate receptor GPR91. Mol. Metab. 2017;6:1585–96. https://doi.org/10.1016/J.MOLMET.2017.09.005.

[13] Krzak G, Willis CM, Smith JA, Pluchino S, Peruzzotti-Jametti L. Succinate receptor 1: an emerging regulator of myeloid cell function in inflammation. Trends Immunol 2021;42:45–58. https://doi.org/10.1016/j.it.2020.11.004.

[14] Vargas SL, Toma I, Jung JK, Meer EJ, Peti-Peterdi J. Activation of the succinate receptor GPR91 in macula densa cells causes renin release. J Am Soc Nephrol 2009;20:1002–11. https://doi.org/10.1681/ASN.2008070740.

[15] McCreath KJ, Espada S, Gálvez BG, Benito M, De Molina A, Sepúlveda P, et al. Targeted disruption of the SUCNR1 metabolic receptor leads to dichotomous effects on obesity. Diabetes 2015;64:1154–67. https://doi.org/10.2337/db14-0346.

[16] Wang T, Xu Y, Yuan Y, Xu P, Zhang C, Li F, et al. Succinate induces skeletal muscle fiber remodeling via SUNCR 1 signaling. EMBO Rep 2019;20:1–16. https://doi.org/10.15252/embr.201947892.

[17] Li YH, Choi DH, Lee EH, Seo SR, Lee S, Cho EH. Sirtuin 3 (SIRT3) regulates α-smooth muscle actin (α-SMA) production through the succinate dehydrogenase-G protein-coupled receptor 91 (GPR91) pathway in hepatic stellate sells. J Biol Chem 2016;291:10277–92. https://doi.org/10.1074/jbc.M115.692244.

[18] Park SY, Le CT, Sung KY, Choi DH, Cho EH. Succinate induces hepatic fibrogenesis by promoting activation, proliferation, and migration, and inhibiting apoptosis of hepatic stellate cells. Biochem Biophys Res Commun 2018;496:673–8. https://doi.org/10.1016/j.bbrc.2018.01.106.

[19] Mills EL, Harmon C, Jedrychowski MP, Xiao H, Garrity R, Tran NV, et al. UCP1 governs liver extracellular succinate and inflammatory pathogenesis. Nat Metab 2021;3:604–17. https://doi.org/10.1038/s42255-021-00389-5.

[20] Le CT, Nguyen G, Park SY, Choi DH, Cho EH. LY2405319, an analog of fibroblast growth factor 21 ameliorates α-smooth muscle actin production through inhibition of the succinate-G-protein couple receptor 91 (GPR91) pathway in mice. PloS One 2018;13:e0192146. https://doi.org/10.1371/JOURNAL.PONE.0192146.

[21] Nguyen G, Park SY, Le CT, Park WS, Choi DH, Cho EH. Metformin ameliorates activation of hepatic stellate cells and hepatic fibrosis by succinate and GPR91 inhibition. Biochem Biophys Res Commun 2018;495:2649–56. https://doi.org/10.1016/J.BBRC.2017.12.143.

[22] Liu XJ, Xie L, Du K, Liu C, Zhang NP, Gu CJ, et al. Succinate-GPR-91 receptor signalling is responsible for nonalcoholic steatohepatitis-associated fibrosis: effects of DHA supplementation. Liver Int 2020;40:830–43. https://doi.org/10.1111/LIV.14370.

[23] Sakai M, Sumiyoshi T, Aoyama T, Urayama K. GPR91 antagonist and TGF-b inhibitor suppressed collagen production of high glucose and succinate induced HSC activation. Biochem Biophys Res Commun 2020;530:362–6. https://doi.org/10.1016/j.bbrc.2020.07.141.

[24] Gu L, Zhang F, Wu J, Zhuge Y. Nanotechnology in drug delivery for liver fibrosis. Front Mol Biosci 2022;8:804396. https://doi.org/10.3389/fmolb.2021.804396.

[25] Yeh MM, Brunt EM. Pathological features of fatty liver disease. Gastroenterology 2014;147:754–64. https://doi.org/10.1053/J.GASTRO.2014.07.056.

[26] Kleiner DE, Brunt EM, Van Natta M, Behling C, Contos MJ, Cummings OW, et al. Design and validation of a histological scoring system for nonalcoholic fatty liver disease. Hepatology 2005;41:1313–21. https://doi.org/10.1002/HEP.20701.

[27] Geubelle P, Gilissen J, Dilly S, Poma L, Dupuis N, Laschet C, et al. Identification and pharmacological characterization of succinate receptor agonists. Br J Pharmacol 2017;174:796–808. https://doi.org/10.1111/bph.13738.

[28] Haffke M, Fehlmann D, Rummel G, Boivineau J, Duckely M, Gommermann N, et al. Structural basis of species-selective antagonist binding to the succinate receptor. Nature 2019;574:581–5. https://doi.org/10.1038/s41586-019-1663-8.

[29] Benveniste R, Danoff TM, Ilekis J, Craig HR. Epidermal growth factor receptor numbers in male and female mouse primary hepatocyte cultures. Cell Biochem Funct 1988;6:231–5. https://doi.org/10.1002/cbf.290060403.

[30] Zarei M, Barroso E, Palomer X, Dai J, Rada P, Quesada-López T, et al. Hepatic regulation of VLDL receptor by PPARβ/δ and FGF21 modulates non-alcoholic fatty liver disease. Mol. Metab. 2018;8:117–31. https://doi.org/10.1016/j.molmet.2017.12.008.

[31] He K, Zhu X, Liu Y, Miao C, Wang T, Li P, et al. Inhibition of NLRP3 inflammasome by thioredoxin-interacting protein in mouse Kupffer cells as a regulatory mechanism for non-alcoholic fatty liver disease development. Oncotarget 2017;8:37657–72. https://doi.org/10.18632/oncotarget.17489.

[32] Yuan Hao Y, Wen Cui W, Lin Gao H, Ye Wang M, Liu Y, Ru Li C, et al. Jinlida granules ameliorate the high-fat-diet induced liver injury in mice by antagonising hepatocytes pyroptosis. Pharm Biol 2022;60:274–81. https://doi.org/10.1080/13880209.2022.2029501.

[33] Fondevila MF, Fernandez U, Heras V, Parracho T, Gonzalez-Rellan MJ, Novoa E, et al. Inhibition of carnitine palmitoyltransferase 1A in hepatic stellate cells protects against fibrosis. J Hepatol 2022;77:15–28. https://doi.org/10.1016/j.jhep.2022.02.003.

[34] Evangelakos I, Schwinge D, Worthmann A, John C, Roeder N, Pertzborn P, et al. Oxysterol 7-α hydroxylase (CYP7B1) attenuates metabolic-associated fatty liver disease in mice at thermoneutrality. Cells 2021:10. https://doi.org/10.3390/cells10102656.

[35] Simón J, Goikoetxea-Usandizaga N, Serrano-Maciá M, Fernández-Ramos D, Sáenz de Urturi D, Gruskos JJ, et al. Magnesium accumulation upon cyclin M4 silencing activates microsomal triglyceride transfer protein improving NASH. J Hepatol 2021;75:34–45. https://doi.org/10.1016/j.jhep.2021.01.043.

[36] Correa PRAV, Kruglov EA, Thompson M, Leite MF, Dranoff JA, Nathanson MH. Succinate is a paracrine signal for liver damage. J Hepatol 2007;47:262–9. https://doi.org/10.1016/j.jhep.2007.03.016.

[37] Diehl J, Gries B, Pfeil U, Goldenberg A, Mermer P, Kummer W, et al. Expression and localization of GPR91 and GPR99 in murine organs. Cell Tissue Res 2016;364:245–62. https://doi.org/10.1007/s00441-015-2318-1.

[38] Single cell type - SUCNR1 - The Human Protein Atlas. n.d. https://www.proteinatlas.org/ENSG00000198829-SUCNR1/single+cell+type. [Accessed 25 September 2022].

[39] Baratta F, D'Erasmo L, Bini S, Pastori D, Angelico F, Del Ben M, et al. Heterogeneity of non-alcoholic fatty liver disease (NAFLD): implication for cardiovascular risk stratification. Atherosclerosis 2022;357:51–9. https://doi.org/10.1016/j.atherosclerosis.2022.08.011.

[40] Li YH, Woo SH, Choi DH, Cho EH. Succinate causes α-SMA production through GPR91 activation in hepatic stellate cells. Biochem Biophys Res Commun 2015;463:853–8. https://doi.org/10.1016/j.bbrc.2015.06.023.

[41] DeZwaan-McCabe D, Riordan JD, Arensdorf AM, Icardi MS, Dupuy AJ, Rutkowski DT. The stress-regulated transcription factor CHOP promotes hepatic inflammatory gene expression, fibrosis, and oncogenesis. PLoS Genet 2013;9:e1003937. https://doi.org/10.1371/JOURNAL.PGEN.1003937.

[42] Samuel VT, Shulman GI. Nonalcoholic fatty liver disease as a nexus of metabolic and hepatic diseases. Cell Metab 2018;27:22–41. https://doi.org/10.1016/j.cmet.2017.08.002.

[43] Feng X, Xiao Y, Guo Q, Peng H, Zhou H-Y, Wang J-P, et al. Parathyroid hormone alleviates non-alcoholic liver steatosis via activating the hepatic cAMP/PKA/CREB pathway. Front. Endocrinol. (Lausanne) 2022;13:899731. https://doi.org/10.3389/fendo.2022.899731.

[44] Gao D, Nong S, Huang X, Lu Y, Zhao H, Lin Y, et al. The effects of palmitate on hepatic insulin resistance are mediated by NADPH oxidase 3-derived reactive oxygen species through JNK and p38 MAPK pathways. J Biol Chem 2010;285:29965–73. https://doi.org/10.1074/jbc.M110.128694.

[45] Marjot T, Moolla A, Cobbold JF, Hodson L, Tomlinson JW. Nonalcoholic fatty liver disease in adults: current concepts in etiology, outcomes, and management. Endocr Rev 2020;41:66–117. https://doi.org/10.1210/ENDREV/BNZ009.

[46] Bedogni G, Bellentani S, Miglioli L, Masutti F, Passalacqua M, Castiglione A, et al. The fatty liver index: a simple and accurate predictor of hepatic steatosis in the general population. BMC Gastroenterol 2006:6. https://doi.org/10.1186/1471-230X-6-33.

[47] Staňková P, Kučera O, Peterová E, Elkalaf M, Rychtrmoc D, Melek J, et al. Western diet decreases the liver mitochondrial oxidative flux of succinate: insight from a murine NAFLD model. Int J Mol Sci 2021;22:6908. https://doi.org/10.3390/ijms22136908.
[48] Khamaysi A, Anbtawee-Jomaa S, Fremder M, Eini-Rider H, Shimshilashvili L, Aharon S, et al. Systemic succinate homeostasis and local succinate signaling affect blood pressure and modify risks for calcium oxalate lithogenesis. J Am Soc Nephrol 2019;30:381–92. https://doi.org/10.1681/ASN.2018030277.
[49] Zhang X, Ji X, Wang Q, Li JZ. New insight into inter-organ crosstalk contributing to the pathogenesis of non-alcoholic fatty liver disease (NAFLD). Protein Cell 2018;9:164–77. https://doi.org/10.1007/s13238-017-0436-0.
[50] Yang Q, Chen X, Zhang Y, Hu S, Hu F, Huang Y, et al. The E3 ubiquitin ligase ring finger protein 5 ameliorates NASH through ubiquitin-mediated degradation of 3-hydroxy-3-methylglutaryl CoA reductase degradation protein 1. Hepatology 2021;0:1–19. https://doi.org/10.1002/hep.32061.
[51] Regard JB, Sato IT, Coughlin SR. Anatomical profiling of G protein-coupled receptor expression. Cell 2008;135:561–71. https://doi.org/10.1016/j.cell.2008.08.040.
[52] An YA, Chen S, Deng Y, Wang ZV, Funcke JB, Shah M, et al. The mitochondrial dicarboxylate carrier prevents hepatic lipotoxicity by inhibiting white adipocyte lipolysis. J Hepatol 2021;75:387–99. https://doi.org/10.1016/j.jhep.2021.03.006.
[53] Villanueva-Carmona T, Cedó L, Madeira A, Ceperuelo-Mallafré V, Rodríguez-Peña M-M, Núñez-Roa C, et al. SUCNR1 signaling in adipocytes controls energy metabolism by modulating circadian clock and leptin expression. Cell Metab 2023;35:601–619.e10. https://doi.org/10.1016/j.cmet.2023.03.004.
[54] Lu B, Bridges D, Yang Y, Fisher K, Cheng A, Chang L, et al. Metabolic crosstalk: molecular links between glycogen and lipid metabolism in obesity. Diabetes 2014;63:2935–48. https://doi.org/10.2337/db13-1531.
[55] An P, Wei LL, Zhao S, Sverdlov DY, Vaid KA, Miyamoto M, et al. Hepatocyte mitochondria-derived danger signals directly activate hepatic stellate cells and drive progression of liver fibrosis. Nat Commun 2020;11:2362. https://doi.org/10.1038/s41467-020-16092-0.
[56] Gao Y, Wang Y, Liu H, Liu Z, Zhao J. Mitochondrial DNA from hepatocytes induces upregulation of interleukin-33 expression of macrophages in nonalcoholic steatohepatitis. Dig Liver Dis 2020;52:637–43. https://doi.org/10.1016/j.dld.2020.03.021.
[57] Barbier L, Robin A, Sindayigaya R, Ducousso H, Dujardin F, Thierry A, et al. Endogenous interleukin-33 acts as an alarmin in liver ischemia-reperfusion and is associated with injury after human liver transplantation. Front Immunol 2021;12:744927. https://doi.org/10.3389/fimmu.2021.744927.
[58] Gao Y, Liu Y, Yang M, Guo X, Zhang M, Li H, et al. IL-33 treatment attenuated diet-induced hepatic steatosis but aggravated hepatic fibrosis. Oncotarget 2016;7:33649–61. https://doi.org/10.18632/oncotarget.9259.
[59] Chen XY, Wang C, Huang YZ, Zhang LL. Nonalcoholic fatty liver disease shows significant sex dimorphism. World J Clin Cases 2022;10:1457–72. https://doi.org/10.12998/wjcc.v10.i5.1457.